CHAOTIC MOTION OF AN ELASTO-PLASTIC BEAM

Marcelo A. Savi
Instituto Militar de Engenharia, Departamento de Engenharia Mecânica e de Materiais
22.290.270 - Rio de Janeiro - RJ - Brasil
E-Mail: savi@epq.ime.eb.br

Pedro Manuel C. L. Pacheco
CEFET/RJ, Departamento de Engenharia Mecânica
20.271.110 - Rio de Janeiro - RJ - Brasil
E-Mail: calas@cefet-rj.br

Abstract. *The non-linear dynamics of a pin-ended elasto-plastic beam is discussed in this contribution. Ideal plasticity is in focus. Free and forced responses are considered. An iterative numerical procedure, based on the operator split technique, is developed. This work shows that jump phenomenon and sensitivity on initial conditions imply that the system response may become unpredictable even when a periodic response is expected. Chaotic motion is also associated with the unpredictability of the beam response.*

Keywords: Chaos, Non-linear dynamics, Elasto-plasticity.

1. INTRODUCTION

This contribution investigates the non-linear dynamics of a pin-ended elasto-plastic beam. The beam is modeled by the Symonds' model where a pin-ended beam with length $2L$, and uniform rectangular cross section of area $A = bh'$, is represented by two rigid links, each of length L, joined by an elasto-plastic element. The two rigid bars are assumed to have mass per unit length ρ, the same as for the uniform beam (Shanley, 1947). The beam model is depicted in Fig.1.

An iterative numerical procedure, based on the operator split technique, is developed. Numerical simulations discuss the free and forced responses of the beam. Some dynamical characteristics of the beam imply that the system response may become unpredictable. Chaotic motion is one of these and it may occur for some parameters. There is also jump phenomenon which implies that small changes in force amplitudes cause great variations in the steady state responses.
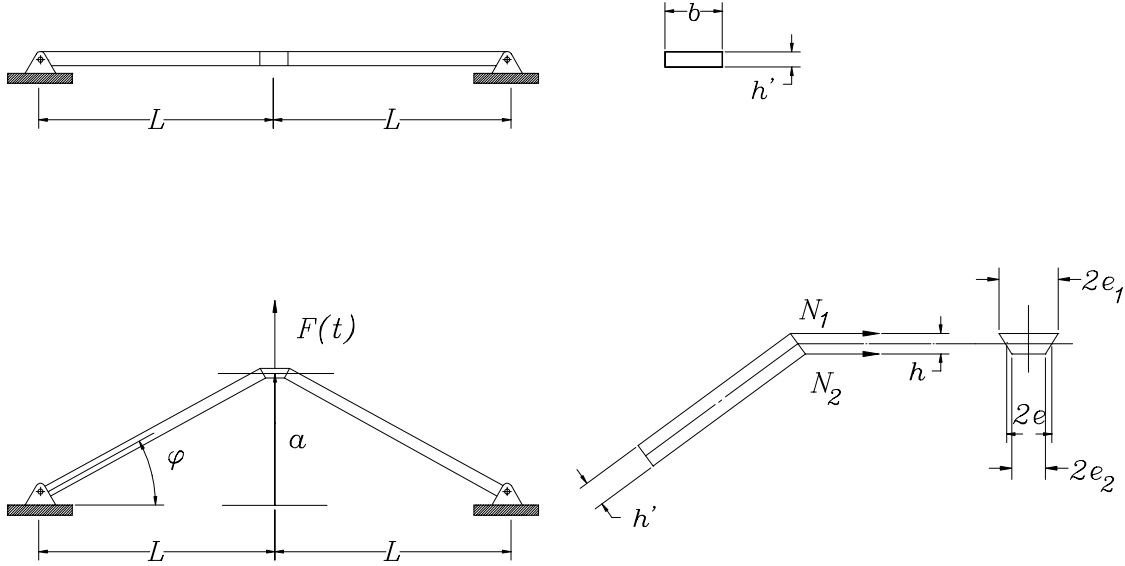
Figure 1 - Elasto-plastic Beam.

2. MODEL FOR AN ELASTO-PLASTIC BEAM

Geometric considerations permit to define the relation between the cell position, a, and the angle of rotation, φ, and also the semi-extension of the cell centerline, e, and the semi-extension of each flange, e_1 and e_2,

$$a = L\sin\varphi$$

$$e = L(\cos\varphi_0 - \cos\varphi)\,, \quad e_1 = e + \frac{h}{2}\sin\varphi\,, \quad e_2 = e - \frac{h}{2}\sin\varphi \ . \tag{1}$$

The constitutive equation for ideal plasticity is given by,

$$\sigma = E(\varepsilon - \varepsilon^p) \quad \text{and} \quad \dot{\varepsilon}^p = \gamma\,\text{sign}(\sigma) \tag{2}$$

where $\text{sign}(\sigma) = \sigma\,/\,|\sigma|$. σ is the one-dimensional stress, ε and ε^p is the total and plastic one-dimensional strain, respectively. γ represents the rate at which plastic deformations take place. E is the Young modulus. The yield function, $h(\sigma)$, the Kuhn-Tucker conditions and the consistency condition are given by (Savi & Pacheco, 1997):

$$h(\sigma) = |\sigma| - \sigma_y$$

$$\gamma \geq 0\,, \quad \gamma h(\sigma) = 0\,, \quad \gamma \dot{h}(\sigma) = 0 \quad \text{if} \quad h(\sigma) = 0\,. \tag{3}$$

Here, σ_y is the yield stress.

The force and moment resultants in the cell are taken by considering the same relations of those of a sandwich beam, consisting of two bars each in simple tension or compression (Symonds & Yu, 1985). Hence,

$$N = N_1 + N_2 = \int_{A_1} \sigma_1 dA + \int_{A_2} \sigma_2 dA$$

$$M = (N_2 - N_1)\frac{h}{2} \tag{4}$$

where N_1 and N_2 are the forces on each flange. Assuming that the total strain on each flange is obtained by dividing the semi-extension by the semi-length of the beam, and the area of each flange is a half of the beam cross section area, hence,

$$N_i = \frac{EA}{2L}(e_i - e_i^p) \ (i = 1,2). \tag{5}$$

where e_i^p is the plastic semi-extension on each flange.

Governing equations of the model are obtained by establishing the equilibrium of moment on the half beam. Neglecting the inertia of the elasto-plastic element, and assuming a linear viscous external dissipation,

$$\ddot{\varphi} + \mu c\,\dot{\varphi} + \mu L\,N \sin\varphi - \mu M = \frac{\mu L}{2} F(t) \tag{6}$$

where $\mu = 3/\rho L^3$ and c is the linear viscous dissipation parameter. N and M are given by equations (1,5). Now, consider the following definitions,

$$\omega_0^2 = \mu L\,N_y \ , \quad c_0 = \mu c/\omega_0 \ , \quad \mu_0 = M_y/L\,N_y \ , \quad f = F/2N_y \ , \quad \tau = \omega_0 t$$

$$n = N/N_y \ , \quad m = M/M_y . \tag{7}$$

Here $N_y = \sigma_y A$ and $M_y = N_y h/2$. Denoting the non-dimensional time derivative by $(\ )' = d(\ )/d\tau$, the following system can be written,

$$y_1' = y_2$$

$$y_2' = -c_0 y_2 - n \sin y_1 + \mu_0 m + f(\tau) \tag{8}$$

Actually, the space of state variables includes more variables than y_1 and y_2 (Poddar *et al.*, 1988), however, the analysis is developed on a subspace of dimension 2 (Savi & Pacheco, 1997). The numerical solution procedure here proposed uses the operator split technique (Ortiz *et al.*, 1983). First, the equations (8) are integrated using any classical scheme, like fourth order Runge-Kutta, assuming that the variables n and m are known parameters. n and m are evaluated by considering an elastic predictor step (trial state), where plastic variable, ε^p, remains constant from the previous time instant. The next step of solution procedure consists on a plastic corrector step where the feasibility of trial state is evaluated using the return mapping algorithm (Simo & Taylor, 1985). An iterative process takes place until the convergence is achieved (Savi & Pacheco, 1997).

2. FREE VIBRATIONS

In this Section, one discusses the free response of the elasto-plastic beam. This is done by letting $f(\tau)$ vanish in the equations of motion (8). In all simulations, one has taken $L = 0.10$m, $b = 0.02$m, $h' = 0.04$m, $h = 0.68h'$, $\rho = 0.216$ kg/m, $E = 120$ GPa, $\sigma_y = 0.3$ GPa (Poddar *et al.*, 1988). The procedure converges with time steps less than $\Delta\tau = 2\pi / 1000\Omega$.

To illustrate the free response, one considers a system with no external dissipation ($c_0 = 0$). Figure 2 presents results from simulations in the form of phase portrait. Different initial conditions cause different plastification of the cell and, as a consequence, alter the position of the equilibrium points in phase space.
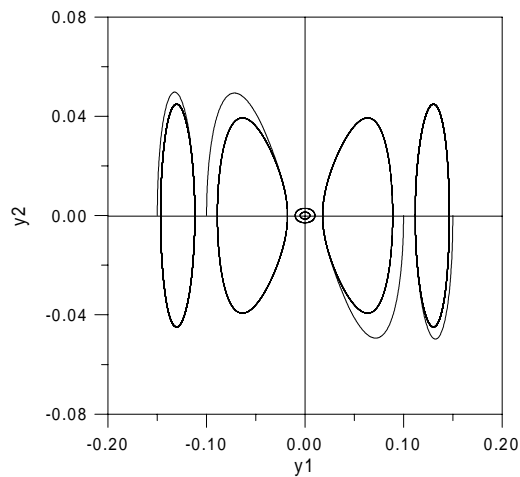

Figure 2 - Phase Portrait.

The beam response presents sensitivity on initial conditions. Poddar *et al.* (1988) show the fractal basin boundaries of the system under free vibration. This conclusion was used to explain the discrepancy among some finite element results shown in Symonds & Yu (1985). Figure 3 shows the steady state envelope of maximum and minimum angular displacement, y_1, for different initial conditions. A null initial angular velocity is considered. Figure 3a considers no external dissipation ($c_0 = 0$), and reproduces the result obtained by Symonds & Yu (1985). It should be pointed out that a global change on the response occurs when initial conditions are on the range from 0.086 to 0.092. By considering an external dissipation, asymptotic behavior is expected. Hence, the response tends to be a closed curve in phase space, and the envelope becomes a line. When $c_0 = 0.2$, global changes are characterized by jumps (Fig.3b). For high values of this parameter, for example $c_0 = 1.5$, global changes do not occur anymore (Fig.3c).
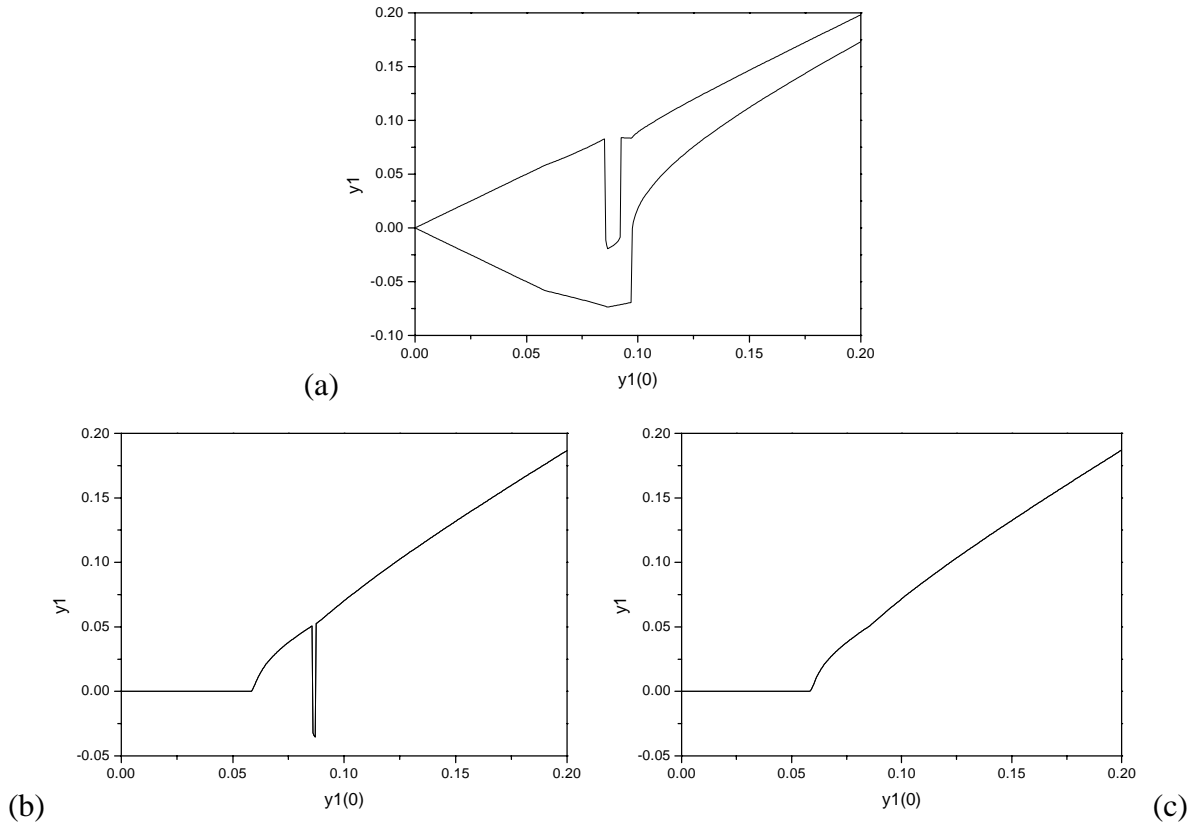
Figure 3 - Steady state envelope of maximum and minimum angular displacement for different initial conditions. (a) $c_0 = 0$; (b) $c_0 = 0.2$; (c) $c_0 = 1.5$.

3. FORCED VIBRATIONS

Forced vibration analysis is now in focus. First, one considers a square wave excitation with amplitude δ. Actually, the considered square wave uses 1% of the period to load or unload. One starts the analysis by considering bifurcation diagrams (Fig.4). The dissipation parameter is $c_0 = 1.5$ and different frequency parameters are considered. The first 30 cycles are neglected.

In order to analyze the jump phenomenon for $\Omega = 1$, one considers two values of forcing amplitude near amplitude $\delta = 0.22$, say $\delta = 0.22$ and $\delta = 0.23$. Figure 5a shows the steady state response for these two situations. For $\Omega = 2$, high values of forcing amplitudes presents different behavior on bifurcation diagram. After jump, which occurs near $\delta = 0.37$, one value of the forcing amplitude is related with many points. This behavior is associated with transient response since the steady state is periodic. Figure 5b shows the steady state response for two forcing amplitudes very close: $\delta = 0.37$ and $\delta = 0.38$. There is a global change on dynamical response.
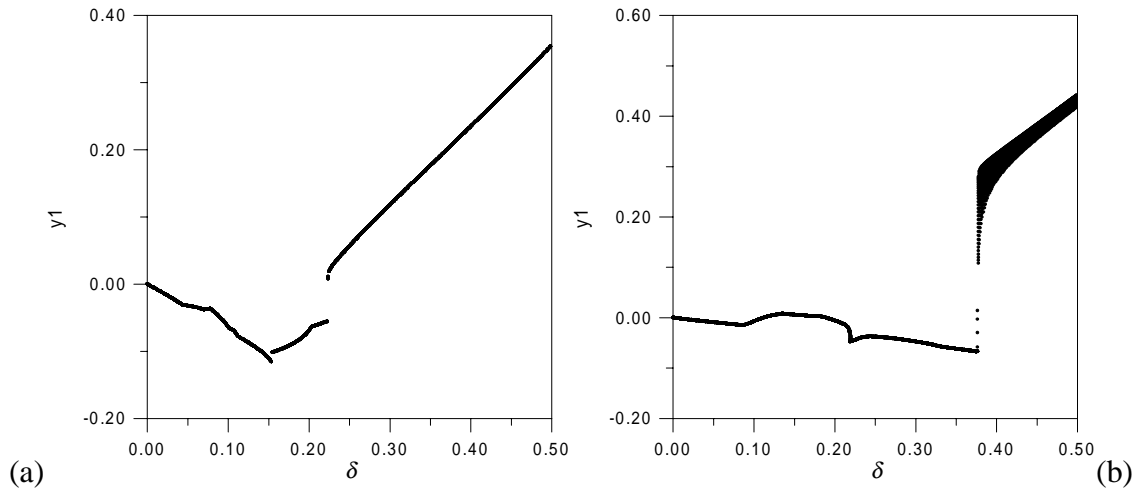
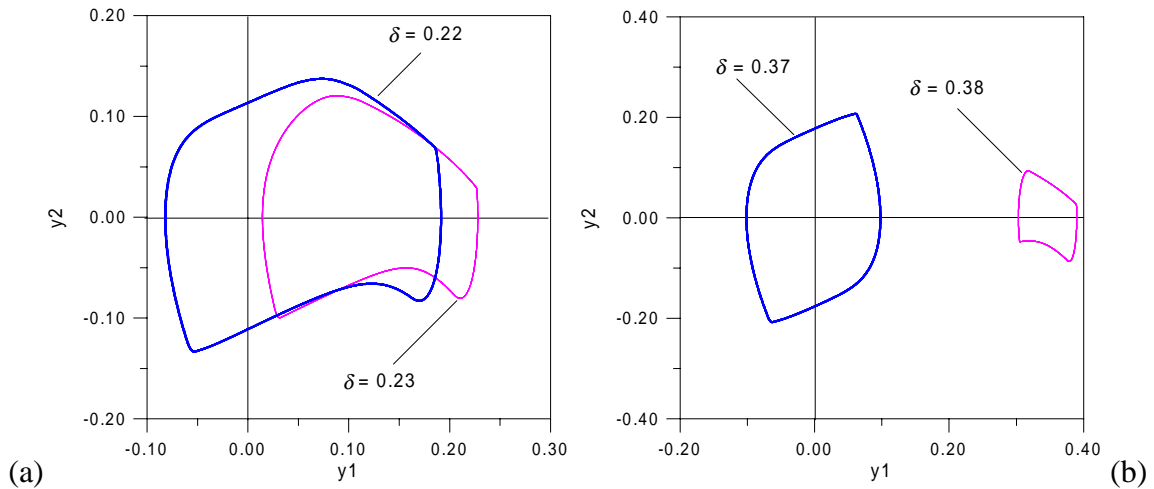Figure 4 - Bifurcation Diagrams. (a) $\Omega = 1$; (b) $\Omega = 2$.

Figure 5 - Steady state response. (a) $\Omega = 1$; (b) $\Omega = 2$.

In spite of the beam does not exhibit chaotic motion with the considered physical parameters, jump phenomenon and sensitivity on initial conditions introduces difficulties to predict the beam behavior. Poddar *et al.* (1988) show that chaotic motion occurs in Symonds' beam when it is subjected to periodic impulses. Hence, it is interesting to consider different parameters to evaluate the possibility of chaotic motion. With this aim, one considers a dissipation parameter $c_0 = 0.2$. Figure 6 shows the bifurcation diagram with frequency parameter $\Omega = 1$. Now, it is possible to identify regions with cloud of points associated with chaos.

The strange attractor of the motion for $\delta = 0.08$ is depicted in Fig.7a, while Fig.7b presents the periodic phase plane for $\delta = 0.04$. The Fast Fourier Transform (FFT) analysis permits to clearly identify the difference between the two responses (Fig.8). As it is well known, the FFT of a chaotic signal presents continuous spectra over a limited range. The energy is spread over a wider bandwidth. On the other hand, the FFT of a periodic signal presents discrete spectra, where a finite number of frequencies contribute for the response (Moon, 1992; Mullin, 1993).
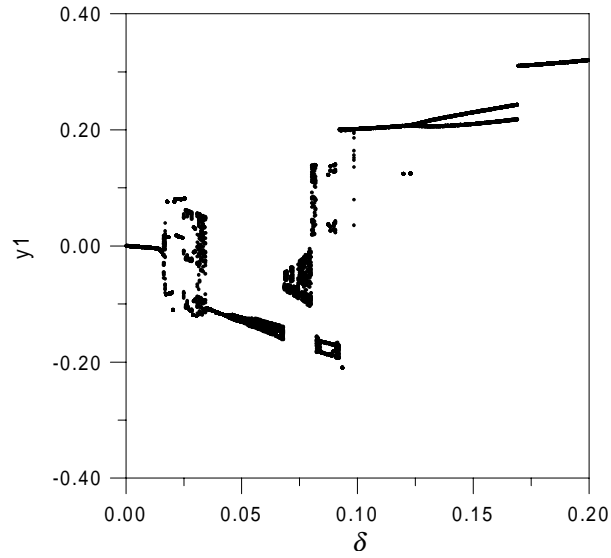
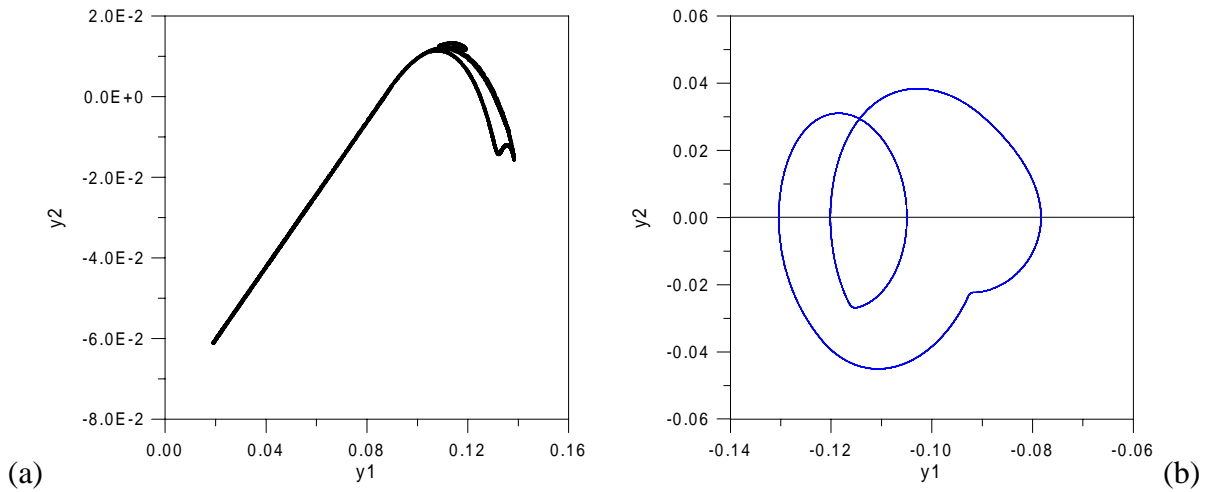Figure 6 - Bifurcation Diagram for $c_0 = 0.2$ and $\Omega = 1$.

(a)

(b)

Figure 7 - Beam response for $\Omega = 1$ and $c_0 = 0.2$.
(a) Strange attractor for $\delta = 0.08$; (b) Phase plane for $\delta = 0.04$.
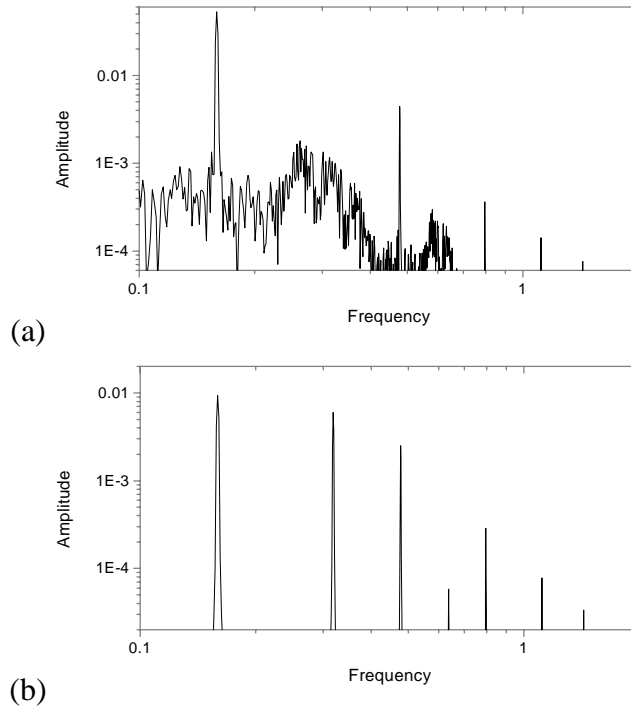
(a)

(b)

Figure 8 - FFT analysis $\Omega = 1$ and $c_0 = 0.2$. (a) Chaotic, $\delta = 0.08$; (b) Periodic, $\delta = 0.04$.

Chaotic motion may also occur when the beam is subjected to a harmonic excitation. In order to analyze this situation, one considers a harmonic sinusoidal excitation, $f(\tau) = \delta \sin(\Omega\tau)$ with a dissipation parameter $c_0 = 0.2$. Figure 9 shows the bifurcation diagram with frequency parameter $\Omega = 1$. As in the previous case, it is possible to identify regions with cloud of points associated with chaos. Figure 10 shows the strange attractor of the motion for $\delta = 0.13$, while Fig.10b presents the periodic phase plane for $\delta = 0.15$. The Fast Fourier Transform (FFT) analysis permits to identify a clearly difference between the two responses (Fig.11).
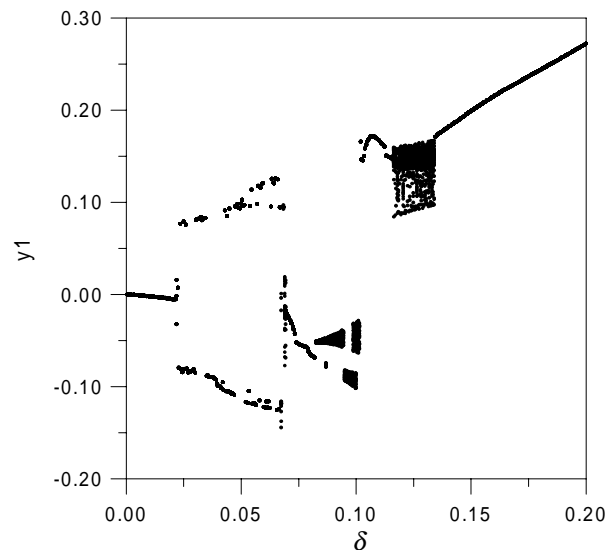

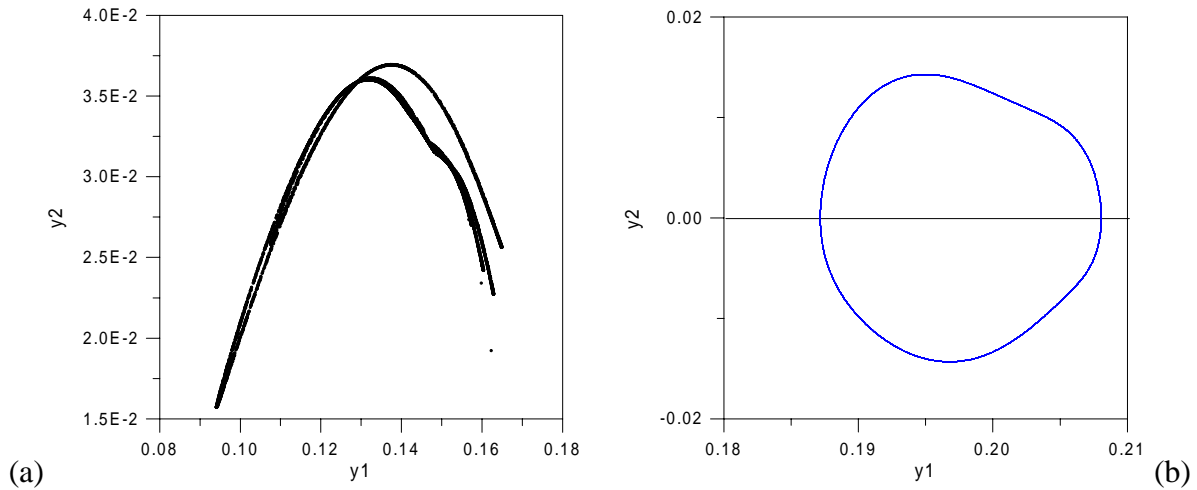Figure 9 - Bifurcation Diagram for $c_0 = 0.2$ and $\Omega = 1$.

(a)   (b)

Figure 10 - Beam response for $\Omega = 1$ and $c_0 = 0.2$.
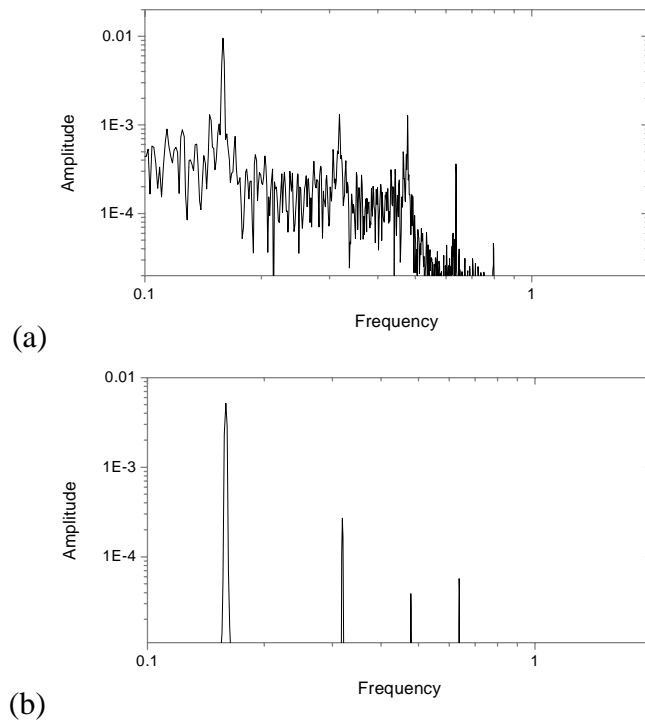Strange attractor for $\delta = 0.13$; (b) Phase plane for $\delta = 0.15$.

(a)

(b)

Figure 11 - FFT analysis $\Omega = 1$ and $c_0 = 0.2$. (a) Chaotic, $\delta = 0.13$; (b) Periodic, $\delta = 0.15$.

4. CONCLUSIONS

A dynamic analysis of a pin-ended elasto-plastic beam, described by the Symonds' model, is considered. Ideal plasticity is focused. The numerical method proposed in this work permits the use of a combination of classical algorithms to evaluate the response of elasto-plastic dynamical systems. Numerical simulations of free and forced vibrations are evaluated. Forced vibrations analysis shows that jump phenomenon occurs for some parameters. In this situation, a very close

change in forcing parameter causes a qualitative change in the beam response. Chaotic motion is also possible in the beam response. These behaviors may cause practical problems to predict the response of the beam, even when periodic response is expected.

REFERENCES

Moon, F.C., 1992, "*Chaotic and Fractal Dynamics*", John Wiley.

Mullin, T., 1993, "*The Nature of Chaos*", Clarendon Press.

Ortiz, M., Pinsky, P.M. & Taylor, R.L., 1983, "Operator Split Methods for the Numerical Solution of the Elastoplastic Dynamic Problem", *Computer Methods in Applied Mechanical Engineering*, Vol. 39, pp. 137-157.

Poddar, B., Moon, F.C. & Mukherjee, S., 1988, "Chaotic Motion of an Elastic-Plastic Beam", *ASME Journal of Applied Mechanics*, Vol. 55, pp. 185-189.

Pratap, R., Mukherjee, S. & Moon, F.C., 1994, "Dynamic Behavior of a Bilinear Hysteretic Elasto-Plastic Oscillator, Part I: Free Oscillations", *Journal of Sound and Vibration*, Vol. 172(3), pp. 321-337.

Pratap, R., Mukherjee, S. & Moon, F.C., 1994, "Dynamic Behavior of a Bilinear Hysteretic Elasto-Plastic Oscillator, Part II: Oscillations Under Periodic Impulse Forcing", *Journal of Sound and Vibration*, Vol. 172(3), pp. 339-358.

Savi, M.A. & Pacheco, P.M.C.L., 1997, "Non-Linear Dynamics of an Elasto-Plastic Oscillator with Kinematic and Isotropic Hardening", *Journal of Sound and Vibration*, Vol. 207(2), pp.207-226.

Shanley, F.R., 1947, "Inelastic Column Theory", *Journal of the Aeronautical Sciences*, Vol. 14, pp. 261-267.

Simo, J.C. & Taylor, R.L., 1985, "Consistent Tangent Operators for Rate-Independent Elastoplasticity", *Computer Methods in Applied Mechanical Engineering*, Vol. 48, pp. 101-118.

Symonds, P.S. & Yu, T.X., 1985, "Counterintuitive Behavior in a Problem of Elastic-Plastic Beam Dynamics", *ASME Journal of Applied Mechanics*, Vol. 52, pp. 517-522.